

# A HYBRID CASCADED MULTILEVEL INVERTER WITH PREDICTIVE CAPACITOR VOLTAGE OF REDUCED COMMON MODE VOLTAGE OPERATION AND INCREASED LINEAR MODULATION

M.Shobana<sup>1</sup>, D.Ramya<sup>2</sup>, K.Vijayakumar<sup>3</sup>, M.Sudhakaran<sup>4</sup>

<sup>1,2</sup>UG Student, Dept. of EEE, Ganadipathy Tulsi's Jain Engineering College, Vellore, India,

<sup>3</sup>Assistant Professor, Dept. of EEE, Ganadipathy Tulsi's Jain Engineering College, Vellore, India,

<sup>4</sup>Associate Professor, Dept. of EEE, Ganadipathy Tulsi's Jain Engineering College, Vellore, India.

## ABSTRACT

For cascaded multilevel inverter topologies with a single DC supply, closed loop capacitor voltage control is necessary for proper operation. This paper presents zero and reduced common mode voltage (CMV) operation of a hybrid cascaded multilevel inverter with predictive capacitor voltage control. Each phase of the inverter is realized by cascading two 3-level flying capacitor inverters with a half bridge module in between. For the presented inverter topology, there are redundant switching states for each inverter voltage levels. By using these switching state redundancies, for every sampling instant, a cost function is evaluated based on the predicted capacitor voltages for each phase. The switching state which minimizes cost function is treated as the best and is switched for that sampling instant. The inverter operates with zero CMV for a modulation index up to 96%. For modulation indices from 96% to 98% the inverter can operate with reduced CMV magnitude ( $V_{dc}/20$ ) and reduced CMV switching frequency using the new space-vector PWM (SVPWM) presented herein. As a result, the linear modulation range is increased to 98% as compared to 96% for zero CMV operation. Simulation and experimental results are presented for the inverter topology for various steady state and transient operating conditions by running an induction motor drive with open loop V/f control scheme.

**Index Terms:** Predictive Control, Induction motor drive, PWM, Multilevel inverter, Common mode voltage, Floating capacitor

## 1. INTRODUCTION

Multilevel inverters result in reduced voltage harmonic distortion and are ideal for low switching frequency high performance medium voltage application, commonly used multilevel inverter topologies are Neutral Point Clamped inverter (NPC), Flying Capacitor inverter (FC). Cascaded H-Bridge inverter (CHB) and hybrid topologies. Hybrid cascaded inverter topologies result in more voltage levels with reduced number of DC supplies and semiconductor devices compared to NPC, FC and CHB. In recent years, model predictive control (MPC) has proved to be a good choice for the control of power converter and motor drive applications. MPC predicts system behavior using a system model and current system state. For multilevel inverters, which have a finite number of switching states, a predictive controller can select the best state from a number of possible states.

A cost function is evaluated for each of the finite states and the state which minimizes the cost function is used for operation. When number of finite states of the system increases, the computation process also

increases for predictive control. In high dynamic performance predictive control algorithm with reduced computations is presented for an asymmetric cascaded H-bridge inverter. a predictive current controller for cascaded H-bridge inverter with reduced computations is presented. FPGA based implementations of MPC algorithms for NPC and CHB inverter topologies are presented in and respectively.

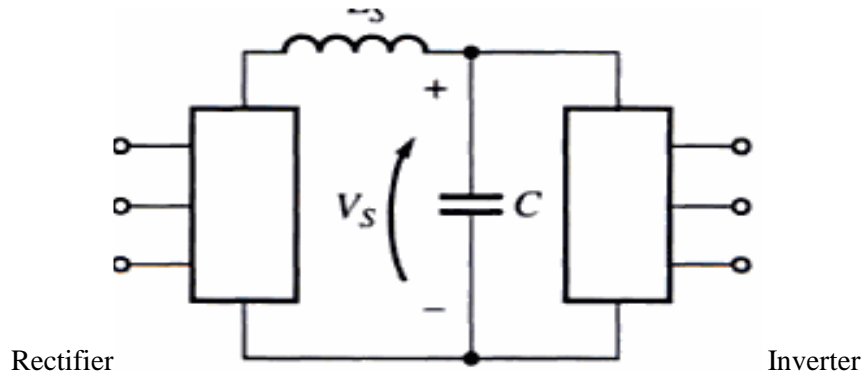


Fig 1. Voltage Source Inverter

Predictive control algorithm is used to minimize the circulating current and balance the DC bus voltage of a modular multilevel inverter topology. Reduced or zero CMV operation is desirable for voltage source inverter fed motor drives to avoid motor bearing failure. By using a modified PWM switching technique, for a two level inverter, the effect of CMV and common mode current (motor bearing current) can be reduced. In multilevel inverter fed motor drive applications, it is possible to make the CMV zero. This is done by selecting voltage space vectors with zero CMV for synthesizing the reference voltage. The disadvantage of zero CMV operation is the reduction in linear modulation range compared to that of normal inverter operation. In a SVPWM technique is presented to extend the linear modulation range of multilevel inverters with reduced CMV switching. In this paper, a cascaded multilevel inverter with a single DC supply is operated with zero and reduced common-mode voltage with a predictive capacitor voltage controller. Floating capacitors are used for generating the multiple voltage levels.

## 2. INVERTER TOPOLOGY

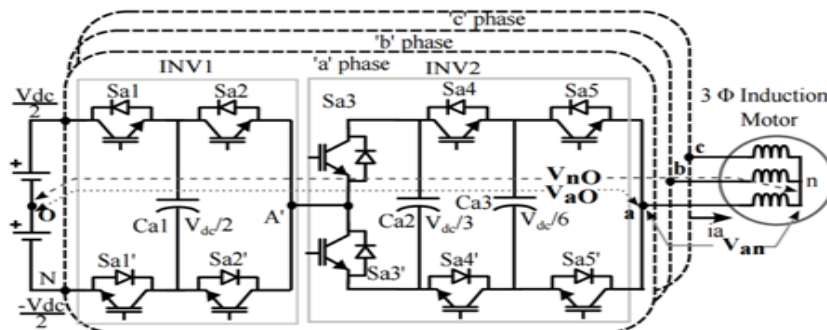
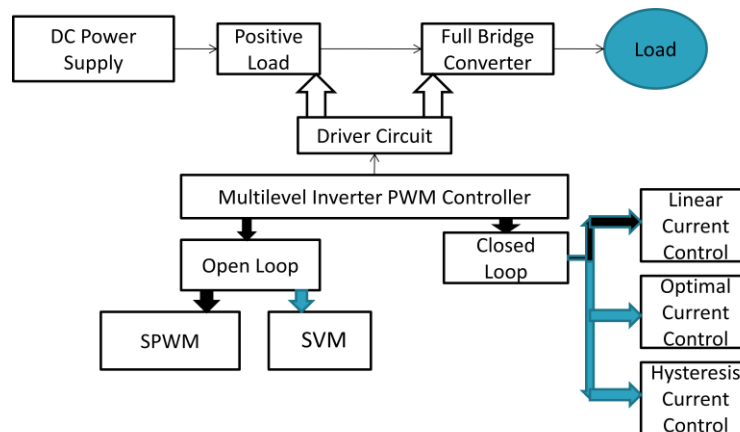


Fig.2 Hybrid Seven Level Inverter Topology

A cost function is evaluated separately for each phase of the inverter to reduce computation time. Also zero and reduced CMV operation of the inverter with SVPWM technique is analyzed. A new space vector PWM technique is proposed for the first time with a reduced CMV magnitude ( $V_{dc}/20$ ) and reduced CMV switching frequency (three times the fundamental frequency). Using this technique, 10% increase in the linear modulation range is achieved compared to zero CMV operation, resulting in improved DC bus utilization.  $V_{aO}$  is defined as inverter pole voltage (voltage between inverter pole 'a' and DC bus mid point 'O'),  $V_{an}$  is defined as motor phase voltage (voltage between inverter pole 'a' and DC motor neutral 'n') and  $V_{nO}$  is defined as common mode voltage (voltage between motor neutral 'n' and DC bus mid point 'O'). Fig. 2 shows the power circuit of a hybrid cascaded multilevel inverter with a single DC supply. The topology consists of five pairs of complementary switches with 32 (25) switching states for each phase. The switches  $S_{x1}$ ,  $S_{x2}$ ,  $S_{x3}$ ,  $S_{x4}$ ,  $S_{x5}$  and  $S_{x10}$ ,  $S_{x20}$ ,  $S_{x30}$ ,  $S_{x40}$ ,  $S_{x50}$  respectively ( $x = a, b, c$  phases) are operated in a complementary manner ( $S_{x1} = 1$  implies  $S_{x10}$  is OFF). The three capacitors ( $C_{x1}$ ,  $C_{x2}$  and  $C_{x3}$ ) per phase are maintained at voltages  $V_{dc}/2$ ,  $V_{dc}/3$ , and  $V_{dc}/6$  respectively. Each phase of the topology can be analysed as a cascaded combination of three-level flying capacitor inverter with a modified five-level flying capacitor inverter. This combination of three-level and five-level inverters can generate eleven voltage levels at 'a', 'b' and 'c' with respect to DC bus mid point 'O'. Seven out of these 11 levels can control capacitor voltages over a switching cycle irrespective of the load power factor and modulation index. This feature can be used for reducing the capacitor size for a given power level. For each of these seven levels. The redundant switching states and effect of these switching states on capacitor charge for a given current direction for phase 'a'. It can be noted that for pole voltage levels  $-V_{dc}/2$  and  $V_{dc}/2$ , all capacitors of that phase are bypassed and hence the voltages are unaffected. For pole voltage levels  $-V_{dc}/3$ , 0, and  $V_{dc}/3$ , there are four redundant switching states, and for pole voltage levels  $-V_{dc}/6$  and  $V_{dc}/6$ , there are five redundant switching states. For the remaining four pole voltages ( $-5V_{dc}/6$ ,  $-4V_{dc}/6$ ,  $4V_{dc}/6$  and  $5V_{dc}/6$ ), the capacitor charging depends on both modulation index and load power factor. This imposes operating limit for the stable operation of inverter and requires special control algorithms to maintain the capacitor voltage. So these pole voltages are not used for the inverter operation presented in this work. In SVPWM with hysteresis band based capacitor voltage control schemes, the capacitor voltages are compared to reference voltages in a hysteresis comparator. At each sampling instant, the controller selects the switching state from a look-up table based on the hysteresis outputs and desired pole voltage. The controller does not consider the present value of capacitor voltage and phase current, and capacitor voltages may cross the hysteresis bands for some load conditions, resulting in higher capacitor voltage ripple. Further, the capacitor voltage dynamics are sensitive to the static look-up table entries.

### 3. BLOCK DIAGRAM

It is the first stage of this project. It gives the DC supply to Inverter. It is obtained from an existing power supply network or from a rotating alternator through a rectifier or a battery, fuel cell, photovoltaic array or magneto hydrodynamic generator.



**Fig.3 Block Diagram of Inverter**

### DC Source Multilevel Inverter

In order to overcome the world excess energy demands, the world trend is replacing the traditional energy sources (TES) which based on non sustainability sources such as fossil fuels and nuclear fission by utilizing new efficient and clean energy resources, that are based on natural sources, such as sunlight power, wind power and geothermal power in addition to ocean energy and bioenergy. All these energy sources decrease carbon emission, and it classified as renewable energy sources (RES).

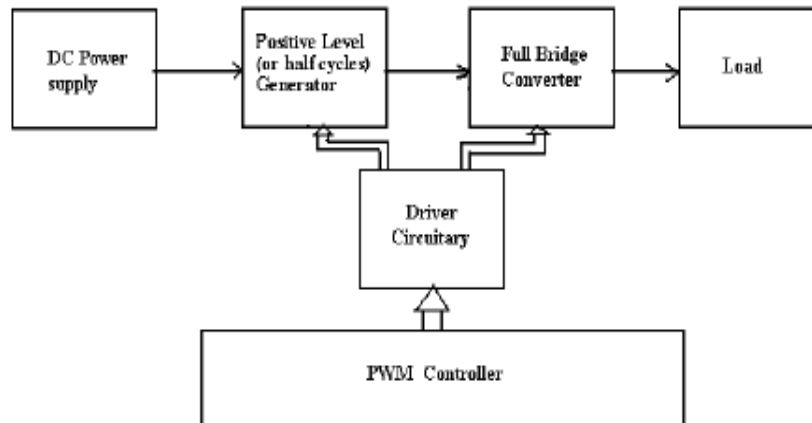


**Fig.4 Block Diagram for DC Source Multilevel Inverter**

### 4. PREDICTIVE CAPACITOR VOLTAGE CONTROL

In predictive control, capacitor voltages for the next sampling instant are predicted using the present capacitor voltages, phase currents and inverter switching functions. To control the dynamics of capacitor voltage, a cost function is evaluated using the predicted capacitor voltages for every redundant switching state. The switching state which minimizes the cost function is switched to generate the inverter pole voltage level. A phase shifting transformer with multiple secondary windings is often utilized mainly for the line current distortions. The rectifier converts

the power supply voltage to a dc voltage with a fixed or variable magnitude. The generally used rectifier topologies include multi-pulse diode or thyristor rectifiers and pulse width modulation (PWM) rectifiers. The dc link can simply be a capacitor that supplies a stiff dc voltage in voltage-source inverters or an inductor that smoothes the dc current in current-source inverters.

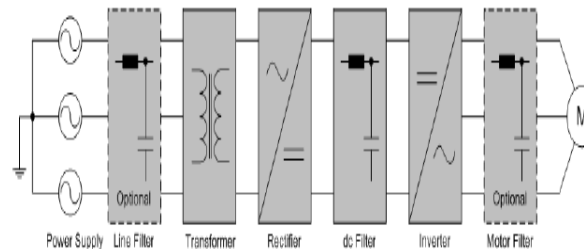


**Fig.5 Typical Block Diagram of Medium Voltage Variable Speed Drives**

For current-source drives, two topologies have found industrial applications in high power ranges: the load-commutated inverter (LCI) and the PWM-CSI. The LCI has been utilized for many years presenting simple converter topology, low manufacturing cost, and reliable operation. Its main problems include low input power factor and distorted input current waveforms, which these problems are overcome by the newer technology of PWM-CSI.

The information about the pole voltage levels to be switched and the time duration of each pole voltage levels to be applied can be obtained from the SVPWM algorithm. The 'a', 'b' and 'c' phase timing signals and the pole voltage transitions over a switching cycle 'Ts'. In general, with SVPWM, the inverter pole voltage of xth phase remains at level 'lx+1' for a duration of 'Tx' and at 'lx' for a duration of 'Ts-Tx'. Using capacitor voltages Vcxk(n) and phase current ix measured at nth sampling instant along with the pole voltage level data and timing information, the capacitor voltage for the duration 'Tx' can be predicted as,

$$V_{cxk} = V_{cxk(n+1)} - V_{cxkref} \quad (1)$$

where V cxkref is the reference voltage of kth capacitor of xth phase. The predictive capacitor voltage control uses a cost function. For zero CMV and reduced CMV operation, the cost function for each phase is evaluated separately. For each phase, by using a separate cost function, phase capacitors are controlled independently and ensures best switching state is selected for each phase. With individual cost function for each phase, the number of computation required also reduces. The number of computation required with single cost function will be (redundancy of 'a' × redundancy of 'a' × redundancy of 'c') compared to (redundancy of 'a' + redundancy of 'b' + redundancy of 'c') with individual cost function. The cost function for each switching state, the optimal switching state for the pole voltage level 'lx+1' can be obtained and all the capacitor voltages can be predicted for the duration 'Tx'. Using this information, optimal switching state for the pole voltage level 'lx' for the duration 'Ts-Tx' also can be obtained.

For nth sampling instant, using level shifted carrier based SVPWM, get the xth phase pole voltage level and timing information for inverter operation. 2) Predict (n+1)th instant capacitor voltage using SVPWM data, previous capacitor voltages and load current. 3) Evaluate the cost function gx for all the

possible switching states for the level data 'lx+1' and 'lx'. Find the switching state which minimizes the cost function  $g_x$  for each phase. 4) Apply the switching state for each phase and repeat the process from step 1 for next sampling instant. Fig. 3 shows the convergence of cost function over time, during motor start-up with all capacitors for phase 'a' initially at 0V. The voltage build-up of capacitors from a relaxed state of 0V for predictive control and hysteresis control it can be seen that the steady state condition (i.e all capacitors are charged to reference) is reached faster with predictive controller than with a hysteresis controller.

### 5. NINE LEVEL INVERTER SPACE VECTOR STRUCTURE AND ZERO CMV LOCATIONS

A seven level inverter has 343 (73) pole voltage combinations which are mapped to 127 space vector locations in the  $\alpha$ - $\beta$  plane. Out of these pole voltage combinations, 37 pole voltage combinations have zero common mode voltage with respect to motor neutral 'n' and DC bus midpoint 'O' ( $V_{nO} = (V_{aO} + V_{bO} + V_{cO})/3$ ). Combining these zero CMV space vector locations, a four level inverter space vector structure rotated 300 anticlockwise is obtained as shown in the Fig. 5. The reference vector ( $\rightarrow V_{ref}$ ) is synthesized by averaging three adjacent vectors using (7 and 8). Analysing the zero CMV space vector structure, maximum peak of fundamental voltage possible is 0.499Vdc compared to 0.577Vdc with normal seven level inverter operation (for 0.577Vdc,  $m = 1$  and 0.499Vdc,  $m = 0.86$ ).

### 6. REDUCED CMV OPERATION TO EXTEND LINEAR MODULATION RANGE

As mentioned in the previous section, with zero CMV operation, DC bus utilization of the inverter gets reduced. In order to get the same torque capability for the induction motor operated with a normal seven level inverter, the DC link voltage needs to be increased for zero CMV operation. Instead of this, by allowing reduced common mode switching, DC bus utilization of inverter is improved compared to zero CMV operation. For the seven level inverter the next CMV near to zero is  $\pm V_{dc}/20$ . For reduced CMV operation presented in this paper, space vector triangles overlap in some regions. This conflict is solved by using the following method.

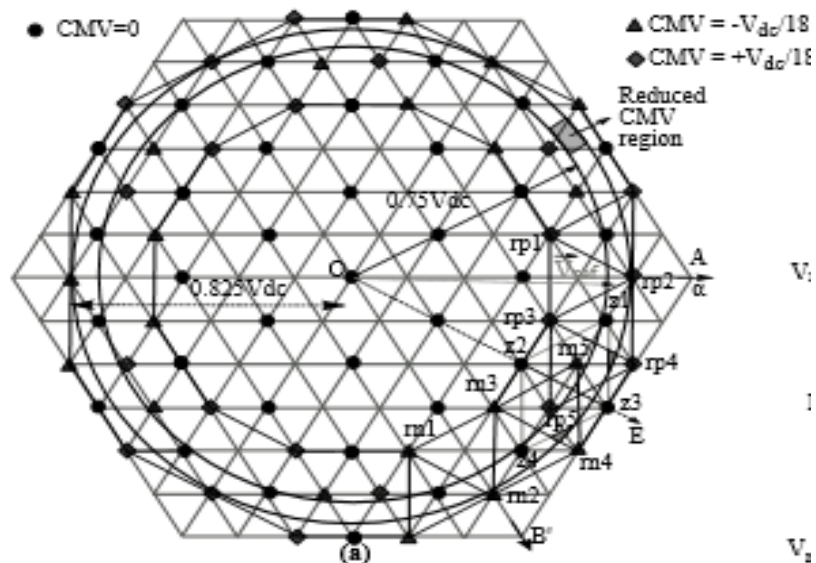


Fig.6 Space vector structure showing reduced CMV

## 7. SIMULATION AND EXPERIMENTAL AND RESULTS

The inverter topology with predictive control is simulated in MATLAB-SIMULINK by modelling the inverter using switching functions. Induction motor is modelled with respect to stator axis reference frame. Various modulation techniques for multilevel power converters are presented. For zero CMV operation ( $m \leq 0.866$ ) presented here, a level shifted carrier based PWM algorithm is used to get the space vector locations and PWM timings. For reduced CMV operation, PWM timings and space vector locations to be switched are obtained using a triangle search algorithm. This algorithm searches one by one all the triangles formed by nearest space vector locations in a sector for positive values of dwell times  $T_0$ ,  $T_1$  and  $T_2$ .

The operation of inverter with predictive capacitor voltage control is tested on a 3 phase induction motor drive with open loop V/f control scheme. Synchronous PWM technique is used for testing the inverter topology. Number of samples per sector is taken as 12 for fundamental frequency ranging from 15 Hz to 25 Hz, 9 for 25 Hz to 37.5 Hz, and 6 for 37.5 Hz to 45 Hz. For fundamental frequency below 15 Hz inverter is operated with a constant switching frequency of 900 Hz. Simulation results under various operating conditions are presented. The zero CMV steady state operation of inverter for fundamental frequencies 10 Hz and 40 Hz the performance of predictive capacitor voltage controller over a hysteresis band based capacitor voltage controller in terms of voltage ripple during no load and full load for fundamental frequencies 10 Hz and 40 Hz with same SVPWM technique.

The frequency spectrum of inverter pole voltage  $V_{aO}$  for reduced CMV operation and normal seven level inverter operation. A 3 phase, 400V, 3.7kW, 50 Hz, 4 pole induction motor drive with open loop V/f control scheme is implemented in hardware for testing the proposed topology. TMS320F28335 DSP is used as the main controller and Xilinx SPARTAN-3 XC3S200 FPGA as the PWM signal generator with a dead time of  $2.5 \mu s$

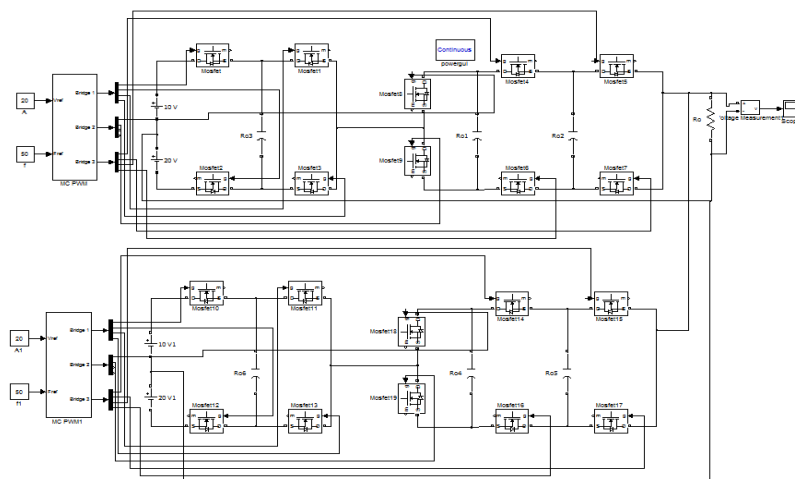
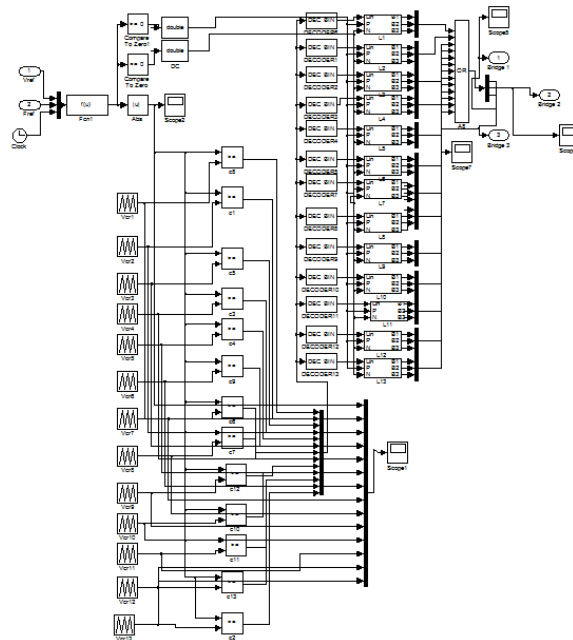
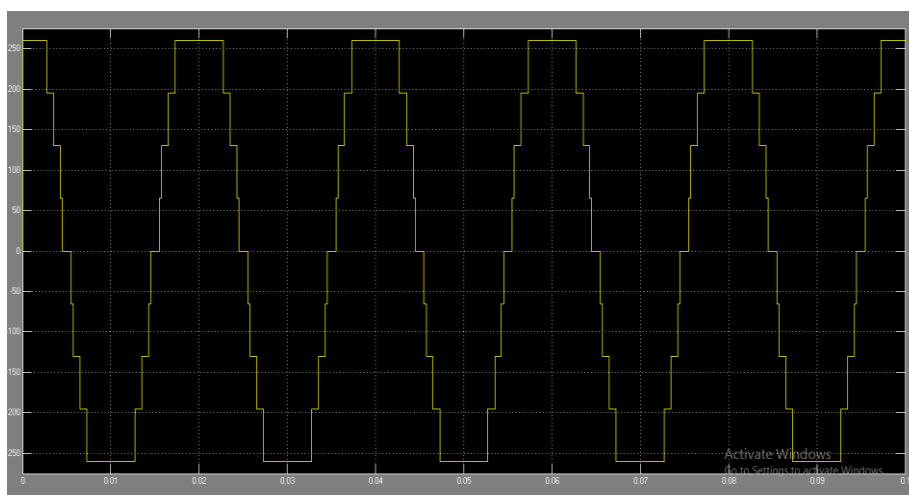


Fig 7. Multilevel inverter for Each Phase



**Fig.8 Circuit Design of Pulse with Modulation**

The maximum voltage that appears across the load resistor is nearly-but never exceeds-500 volts, as result of the small voltage drop across the diode. In the bridge rectifier shown in view B, the maximum voltage that can be rectified is the full secondary voltage, which is 1000 volts. Therefore, the peak output voltage across the load resistor is nearly 1000 volts. With both circuits using the same transformer, the bridge rectifier circuit produces a higher output voltage than the conventional full-wave rectifier circuit.



**Fig.9 Voltage waveform**

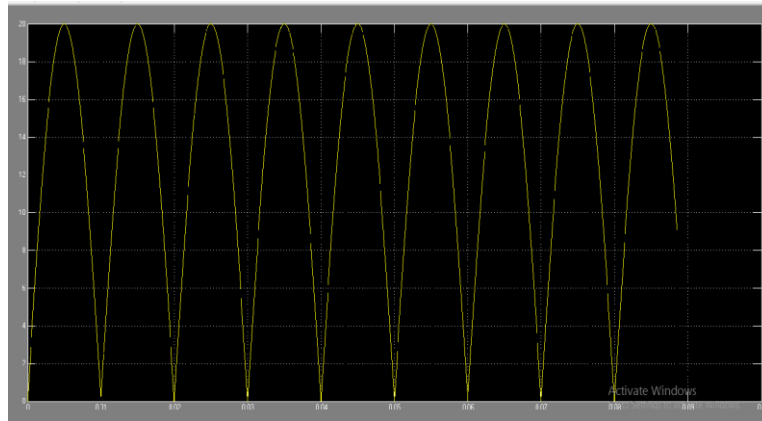


**Fig.10 Input voltage waveform**

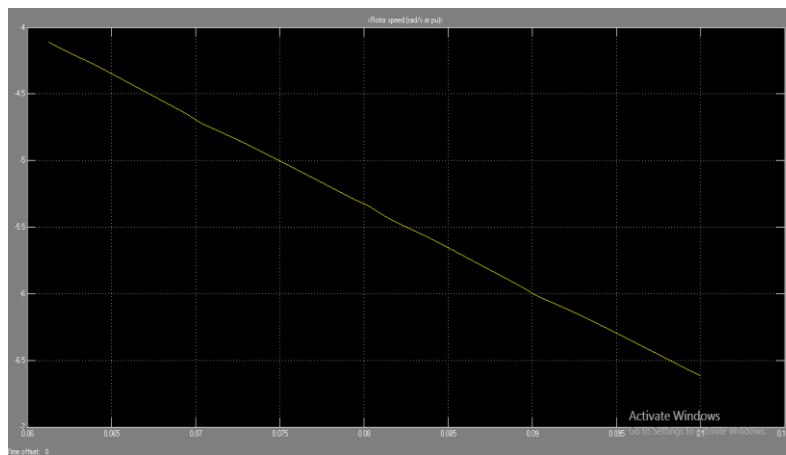


**Fig.11 Rotor speed**

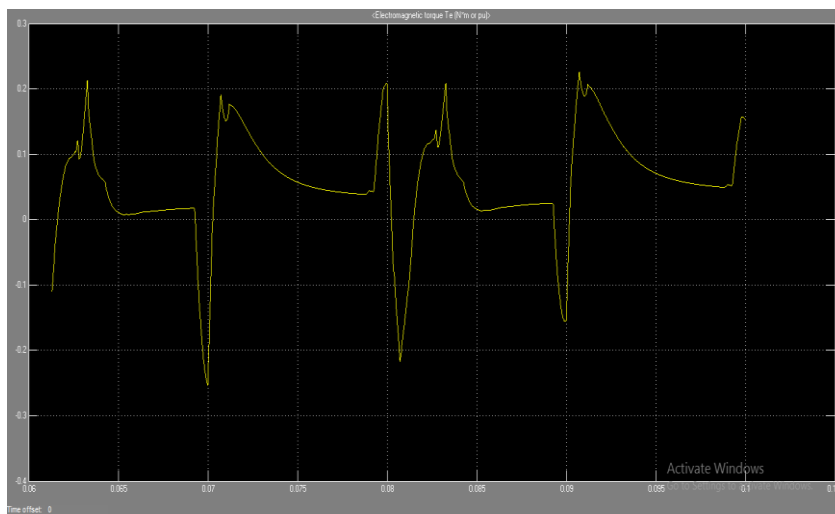


**Fig.12 Rotor Torque**

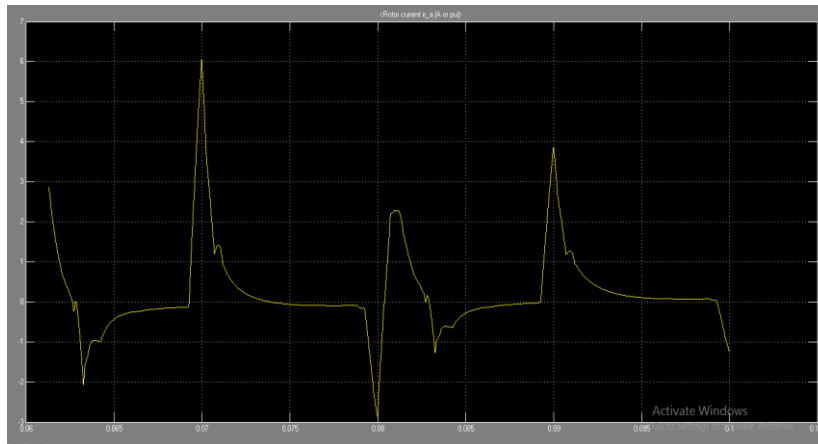


**Fig.13 Rotor Current**

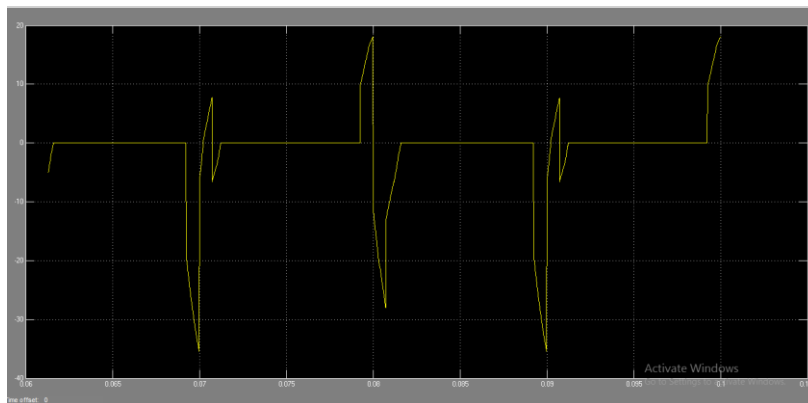


**Fig.14 Total output current waveform**

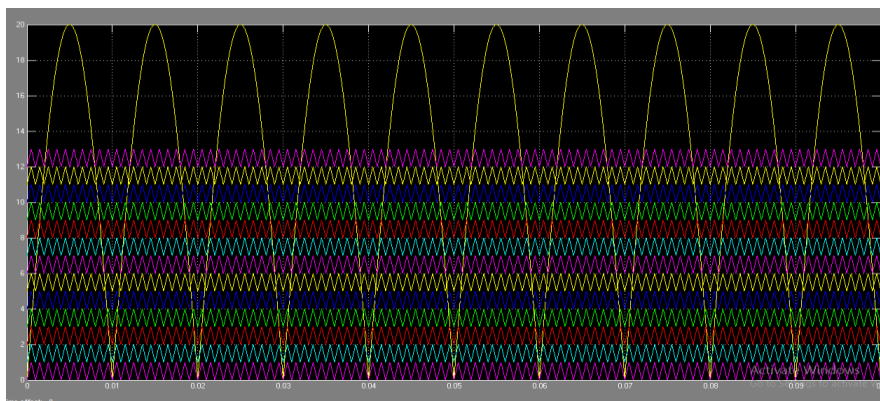


**Fig.15 Total Harmonic distortions waveform**

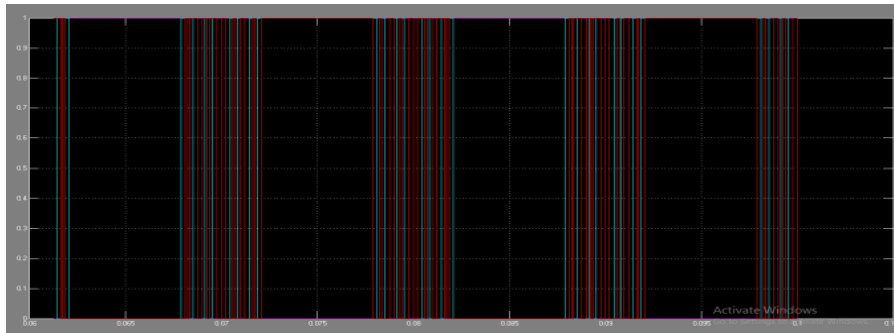


Fig.16 SPWM filtered line voltage



Fig.17 Cascaded Multilevel Inverter

## CONCLUSION

The hybrid PWM techniques for one level inverter are proposed in this project. The proposed space vector hybrid PWM leads to lowest distortion in its class of PWM at any given modulation index for a given average switching frequency. The hybrid PWM is compared to the sinusoidal PWM technique. The results of SPWM are compared with SVPWM. The proposed techniques lead to about reduction in line current distortion over SPWM at the rated voltage and rated frequency of the drive. The superior performance of the proposed techniques over SPWM and existing PWM techniques has been demonstrated using simulation. Hybrid PWM will be further carried out in aim of reducing THD and hardware of the system will be done to verify the simulation results in real time.

## REFERENCES

- [1] S. Kouro, M. Malinowski, K. Gopakumar, J. Pou, L. G. Franquelo, B. Wu, J. Rodriguez, M. A. Perez, and J. I. Leon, "Recent advances and industrial applications of multilevel converters," IEEE Trans. Ind. Electron, vol. 57, no. 8, pp. 2553–2580, Aug 2010.

- [2] H. Abu-Rub, J. Holtz, J. Rodriguez, and G. Baoming, "Medium-voltage multilevel converters-state of the art, challenges, and requirements in industrial applications," *IEEE Trans. Ind. Electron*, vol. 57, no. 8, pp. 2581–2596, Aug 2010.
- [3] J. D. Barros, J. F. A. Silva, and . G. A. Jesus, "Fast-predictive optimal control of npc multilevel converters," *IEEE Trans. Ind. Electron*, vol. 60, no. 2, pp. 619–627, Feb 2013.
- [4] J. Amini, "An effortless space-vector-based modulation for n -level flying capacitor multilevel inverter with capacitor voltage balancing capability," *IEEE Trans. Power Electron*, vol. 29, no. 11, pp. 6188–6195, Nov 2014.
- [5] S. Thielemans, T. J. Vyncke, and J. Melkebeek, "Weight factor selection for model-based predictive control of a four-level flying-capacitor inverter," *IET Power Electronics*, vol. 5, no. 3, pp. 323–333, March 2012.
- [6] S. Choi and M. Saeedifard, "Capacitor voltage balancing of flying capacitor multilevel converters by space vector pwm," *IEEE Trans. Power Delivery*, vol. 27, no. 3, pp. 1154–1161, July 2012.
- [7] M. A. Perez, P. Cortes, and J. Rodriguez, "Predictive control algorithm technique for multilevel asymmetric cascaded h-bridge inverters," *IEEE Trans. Ind. Electron*, vol. 55, no. 12, pp. 4354–4361, Dec 2008.
- [8] P. Cortes, A. Wilson, S. Kouro, J. Rodriguez, and H. Abu-Rub, "Model predictive control of multilevel cascaded h-bridge inverters," *IEEE Trans. Ind. Electron*, vol. 57, no. 8, pp. 2691–2699, Aug 2010.
- [9] T. Geyer and S. Mastellone, "Model predictive direct torque control of a five-level anpc converter drive system," *IEEE Trans. Ind. Appl*, vol. 48, no. 5, pp. 1565–1575, Sept 2012.
- [10] P. R. Kumar, P. P. Rajeevan, K. Mathew, K. Gopakumar, J. I. Leon, and L. G. Franquelo, "A three-level common-mode voltage eliminated inverter with single dc supply using flying capacitor inverter and cascaded h-bridge," *IEEE Trans. Power Electron*, vol. 29, no. 3, pp. 1402–1409, March 2014.
- [11] A. K. Gupta and A. M. Khambadkone, "A space vector modulation scheme to reduce common mode voltage for cascaded multilevel inverters," *IEEE Trans. Power Electron*, vol. 22, no. 5, pp. 1672–1681, Sept 2007.
- [12] M. Malinowski, K. Gopakumar, J. Rodriguez, and M. A. Perez, "A survey on cascaded multilevel inverters," *IEEE Trans. Ind. Electron*, vol. 57, no. 7, pp. 2197–2206, July 2010.
- [13] M. Saeedifard, P. M. Barbosa, and P. K. Steimer, "Operation and control of a hybrid seven-level converter," *IEEE Trans. Power Electron*, vol. 27, no. 2, pp. 652–660, Feb 2012.
- [14] P. Cortes, M. P. Kazmierkowski, R. M. Kennel, D. E. Quevedo, and J. Rodriguez, "Predictive control in power electronics and drives," *IEEE Trans. Ind. Electron*, vol. 55, no. 12, pp. 4312–4324, Dec 2008. [15] P. M. Sanchez, O. Machado, E. J. B. Pea, F. J. Rodriguez, and F. J. Meca, "Fpga-based implementation of a predictive current controller for power converters," *IEEE Trans. Ind. Info*, vol. 9, no. 3, pp. 1312–1321, Aug 2013.
- [16] R. O. Ramirez, J. R. Espinoza, P. E. Melin, M. E. Reyes, E. E. Espinosa, C. Silva, and E. Maurelia, "Predictive controller for a three-phase/singlephase voltage source converter cell," *IEEE Trans. Ind. Info*, vol. 10, no. 3, pp. 1878–1889, Aug 2014
- [17] M. A. Perez, J. Rodriguez, E. J. Fuentes, and F. Kammerer, "Predictive control of ac-ac modular multilevel converters," *IEEE Trans. Ind. Electron*, vol. 59, no. 7, pp. 2832–2839, July 2012.
- [18] S. Chen, T. A. Lipo, and D. Fitzgerald, "Source of induction motor bearing currents caused by pwm inverters," *IEEE Trans. Energy Convers*, vol. 11, no. 1, pp. 25–32, Mar 1996.

- [19] D. Busse, J. Erdman, R. J. Kerkman, D. Schlegel, and G. Skibinski, "Bearing currents and their relationship to pwm drives," IEEE Trans. Power Electron, vol. 12, no. 2, pp. 243–252, Mar 1997.
- [20] M. Cacciato, S. Caro, G. Scarcella, G. Scelba, and A. Testa, "Improved space-vector modulation technique for common mode currents reduction," IET Power Electronics, vol. 6, no. 7, pp. 1248–1256, August 2013.